A comparison of cold spray technique to single particle micro-ballistic impacts for the deposition of polymer particles on polymer substrates

Zahra Khalkhali, Wanting Xie, Victor K. Champagne, Jae-Hwang Lee, Jonathan P. Rothstein

PII: S0257-8972(18)30754-0
DOI: doi:10.1016/j.surfcoat.2018.07.053
Reference: SCT 23619

To appear in: *Surface & Coatings Technology*

Received date: 23 May 2018
Revised date: 16 July 2018
Accepted date: 17 July 2018

Please cite this article as: Zahra Khalkhali, Wanting Xie, Victor K. Champagne, Jae-Hwang Lee, Jonathan P. Rothstein , A comparison of cold spray technique to single particle micro-ballistic impacts for the deposition of polymer particles on polymer substrates. Sct (2018), doi:10.1016/j.surfcoat.2018.07.053

A Comparison of Cold Spray Technique to Single Particle Micro-Ballistic Impacts for the Deposition of Polymer Particles on Polymer Substrates

Zahra Khalkhali[1]*, Wanting Xie[1]*, Victor K. Champagne[2], Jae-Hwang Lee[1] and Jonathan P. Rothstein[1]

*Contributed equally

[1] Department of Mechanical and Industrial Engineering, University of Massachusetts, Amherst, Massachusetts, 01002, USA
[2] United States Army Research Laboratory, Aberdeen Proving Ground, Maryland, 21005, USA

Abstract

A laboratory-scale cold spray system with the capability of accelerating 10 – 100μm polymer particles up to Mach 2 was used to deposit polystyrene and polyamide particles on a variety of different substrates for both cases of like-on-like deposition and deposition onto a melt-cast low-density polyethylene (LDPE) substrate. By systematically varying the particle temperature and impact velocity, the deposition window was developed for each particle and substrate combination in order to understand the cold spray processing conditions necessary to form coatings. The results were compared to those of the micro-ballistic single particle impact experiments. In the latter technique, an ablation laser pulse was used to accelerate a single polymer particle to over 400m/s while being tracked during flight and rebound from the substrate using ultrafast laser photography. Single particle impact studies provide information about the particle impact dynamics including the plastic deformation of a successfully deposited particles and the coefficient of restitution of a rebounding particle that cannot be monitored during cold spray. Particles of both polyamide and polystyrene were found to deposit on a soft LDPE substrate at similar impact velocities using both deposition techniques. A number of differences between the two techniques were also observed. Like-on-like deposition was only found to be successful in cold spray. Additionally, when single particle impacts successfully deposited, the efficiency of deposition was close to 100%, while for the cold spray processes the deposition was less than 5%. These results suggest multiple particle impacts and/or surface roughness can play a major role in the effectiveness and efficiency of the cold spray deposition process for polymers.

Keywords: Window of deposition; Cold spray; Single particle impact test; Critical velocity

1. Introduction

Cold spray is a solid-state coating process that uses a high-speed gas jet to accelerate solid powder particles toward a substrate [1, 2]. Upon impact with the substrate, the particles plastically deform and form strong chemical and/or mechanical bonds with the substrate to form a strong, homogeneous coating with properties comparable to the original powder and little to no porosity. The main advantage of this process over other additive manufacturing and coating techniques like plasma spray, high velocity oxygen fuel, or laser cladding is that melting is avoided in this method which minimizes chances of oxidation and evaporation and hinders mismatches between microstructure, expansion and other properties [2, 3]. Additionally, a technical advantage of the cold spray process, similar to thermal spray, is that the spraying gun can be held by a robot arm and the substrate can be mounted on a 3D printing platform to form complex structures [4]. Cold spray has evolved into a viable additive manufacturing solution, especially for an increasing number of non-traditional applications, such as in the aerospace industry where it has been adapted for the repair and reconditioning of metal parts and components [8]. Cold spray of polymers and polymeric composites has also been used recently to fabricate biocompatible and antibacterial coatings [5]. Additionally, as environmental, health and safety regulations are becoming progressively more stringent, interest in cold spray has grown as a potentially greener alternative because of the lack of solvents in the processing.

Since the onset of cold spray application in mid-1980s, copper, aluminum, nickel, iron, zinc, tin, and alloys of these elements have been studied extensively [2, 6 – 8]. There are also many studies of metallization of polymer substrates using cold spray technique, including tin cold-sprayed onto the surface of polystyrene, polyamide-6, and polypropylene or aluminum cold-sprayed onto carbon reinforced Polyether ether ketone (PEEK) [4] and copper onto Polyvinyl chloride (PVC) and other polymers [9 – 11]. However, investigations on the cold spray deposition of polymer particles on polymer substrates are very sparse and few [12 – 15]. One obstacle that researchers face in their investigations on polymers, is the low deposition efficiency obtained in this process. For example, in the work of Y. Xu et al. [14] less than 1% of the polymer particles were found to adhere to the surface. This is quite different from the observations in metal cold spray where close to 100% deposition efficiency is achieved [8]. In our previous work, we optimized the deposition efficiency for HDPE particles and were able to

increase it to nearly 10% by modifying process variables including nozzle geometry, powder flowrate, carrier gas properties, particle temperature, substrate temperature and particle impact velocity [15]. In this study, our aim is to better understand the role of these process parameters by comparing cold spray deposition to micro-ballistic single particle impacts where the particle flight and rebound can be observed through high speed photography and the deformation and final state of particles after deposition can be observed through electron microscopy.

In metallic cold spray, it has been argued that the strong shear flow formed at the interface between the impacting particle and the substrate can remove the oxide layer from the particle/substrate interface allowing for a strong metallurgical bond to form between the freshly exposed surfaces. In the cold spray deposition of most polymer particles, the formation of metallic bonds is not possible. As a result, other bonding mechanisms such as mechanical interlocking [4], crack filling [16], particle/substrate modulus difference [17], interfacial flow instability [18], and adiabatic shear instability [19] are most likely responsible for particle adhesion. The adiabatic shear instability is regarded as the dominant bonding mechanism when significant plastic deformation occurs during impact as is the case for polymer particles [19]. The adiabatic assumption hypothesizes that the heat generated from the impact-induced plastic deformation does not diffuse far from regions of high deformation and subsequently the high shear can dramatically increase the interfacial temperature between the particle and the substrate. For plastic particles, this adiabatic assumption is reasonable due to the low thermal conduction of the polymer. The elevated temperature, in turn, leads to thermal softening which allows for more plastic deformation and energy dissipation. The adiabatic shear instability can lead to mechanical interlocking and mixing between the particle and the substrate resulting in particle adhesion due to an interfacial flow instability between two materials of different viscosities [18] [21]. Closer examination of the interface between the substrate and the adhered particle is still needed in order to conclusively determine the dominant bonding mechanism in the cold spray deposition of polymers. Monitoring the evolution of the flattening ratio and the crater depth during the impact of cold sprayed polymer powders would be quite helpful in understanding the bonding mechanism. Unfortunately, these experiments are quite difficult because of the large number of particles depositing during cold spray and the peening effect of the subsequent successful and

unsuccessful particle impacts. Here, again single particle impact studies can lead to insights into the impact and adhesion of particles during the cold spray process.

In this study, cold spray deposition and single particle impact experiments of polyamide 12 and polystyrene particles for both cases of like-on-like deposition and deposition on low-density polyethylene were performed to further explore the adhesion process of polymer particles impacting a polymer substrate. We will show that single particle impact studies can provide some valuable insights to the particle deposition process and highlight intriguing differences between single particle and multiple particle impacts.

2. Materials and Methods

A laboratory-scale cold spray system using a consumer grade single-stage air compressor with the capability of accelerating particles up to Mach 2 was used to deposit polystyrene particles with an average diameter of D = 40μm and polyamide 12 (PA) particles with an average diameter of D = 50μm. The polymer cold spray system is described in detail in Bush et al. [15]. It was designed to use either a compressed nitrogen cylinder or a 1.85kW consumer-grade single-stage air compressor capable of producing a pressure of 6.2 bars at 8.5 m^3/hr. The compressed air traveled through filters and a pressure regulator before entering a heated pressure vessel which housed the powder feeder. The hot gas/powder mixture then exited the vessel and passed through the nozzle. The powder and process gas are heated together and mixed well upstream of the nozzle.

The aluminum pressure vessel was heated with three 500W band heaters (Omega MB-1). The temperature of the pressure vessel was monitored with an internal bore thermocouple (Omega BT) inserted through a radial pressure fitting near the bottom of the barrel and was controlled with a PID temperature controller (Omega CN2110). The inner diameter of the pressure vessel was 38mm and it had a total length 27cm. Nozzle inlet conditions were monitored via a thermocouple and a pressure transducer (Omega PX309-300GV) inserted just upstream of the nozzle as seen in Figure 1a. A schematic diagram of the cold spray setup used in this study is shown in Figure 1a, alongside a picture of the actual cold spray system in Figure 1b [15]. The powder feed was accomplished by routing the carrier air around a vibratory powder dispenser contained in the pressure vessel. A pneumatic vibrator (Cleveland Vibrators VM-25)

was mounted on a connecting rod above the pressure vessel. The connecting rod ran through a slip-fit bushing and into the vessel, where it transmitted vibration to an attached aluminum tube that contained the powder to be deposited. The bottom of the tube was capped with coarse wire mesh, which allowed agitated powder to fall into the surrounding carrier gas.

A temperature-controlled 2D xy-stage operated by an open source software package designed for 3D printing (Repetier-Host) was used to move the substrate underneath the nozzle exit at controlled speeds to create deposition patterns consisting of 1D lines and 2D square patterns. Here all 2D deposition patterns were 2cm × 2cm squares that required multiple passes to deposit with 25% overlap between sequential lines (the overlap percentage is true for specific conditions of particle size, velocity and flowrate of about 50μm, 150m/s and 35g/min, respectively). For both the PA and PS particles, deposition was studied on substrates melt-cast from either the polystyrene or polyamide particles to test like-on-like deposition or substrates melt-cast from LDPE to study deposition on a substrate with a different modulus. For simplification, in presenting the results of these experiments, we will use the abbreviation PS-on-LDPE, PS-on-PS, PA-on-LDPE, and PA-on-PA, respectively

A one-dimensional (1D) inviscid compressible flow model of the gas and particle dynamics created by Champagne et al. [22, 23] was used to calculate the velocity, temperature, and pressure variations through the nozzle. It was assumed that the particles do not disturb the flow field. The particle impact velocity and temperature were then calculated using a simple drag law and a lumped capacitance heat transfer model as outlined in Bush et al. [15]. In order to calculate the impact velocity and temperature of the particles, information about the particle diameter along with values of the gas velocity, temperature and pressure along the nozzle were needed.

In the micro-ballistic single particle impact experiments, an ablation laser pulse (5 – 8ns pulse duration, 1064 nm) was created by using a neodymium-doped yttrium aluminum garnet, Nd:YAG laser medium (Quanta-Ray INDI-40-10-HG, Spectra-Physics) to accelerate an individual polymer particle placed near the focal point of the laser ablation on a polydimethylsiloxane (PDMS)/Au/glass substrate. This process is shown schematically in Figure 1c. The particle was subsequently accelerated by the rapid expanding motion of an 80μm thick elastomeric film made of cross-linked PDMS. Combining a femtosecond laser source with three

electro-optic modulators, this micro-ballistic single particle impact experiment, can provide up to 40 million frames per second. A photonic crystal fiber (SCG-800, Newport) was used to convert the gated laser pulses to white light, resulting in an image like the one seen in Figure 1d, containing multiple exposure of the particle in flight as it approaches and rebounds off the substrate. The particle diameter and velocity were measured directly from the ultrafast photograph. Both the PA and PS particles were successfully accelerated in the micro-ballistic system and impacted on both like-on-like substrates of melt cast PS and PA and on a melt cast LDPE substrate.

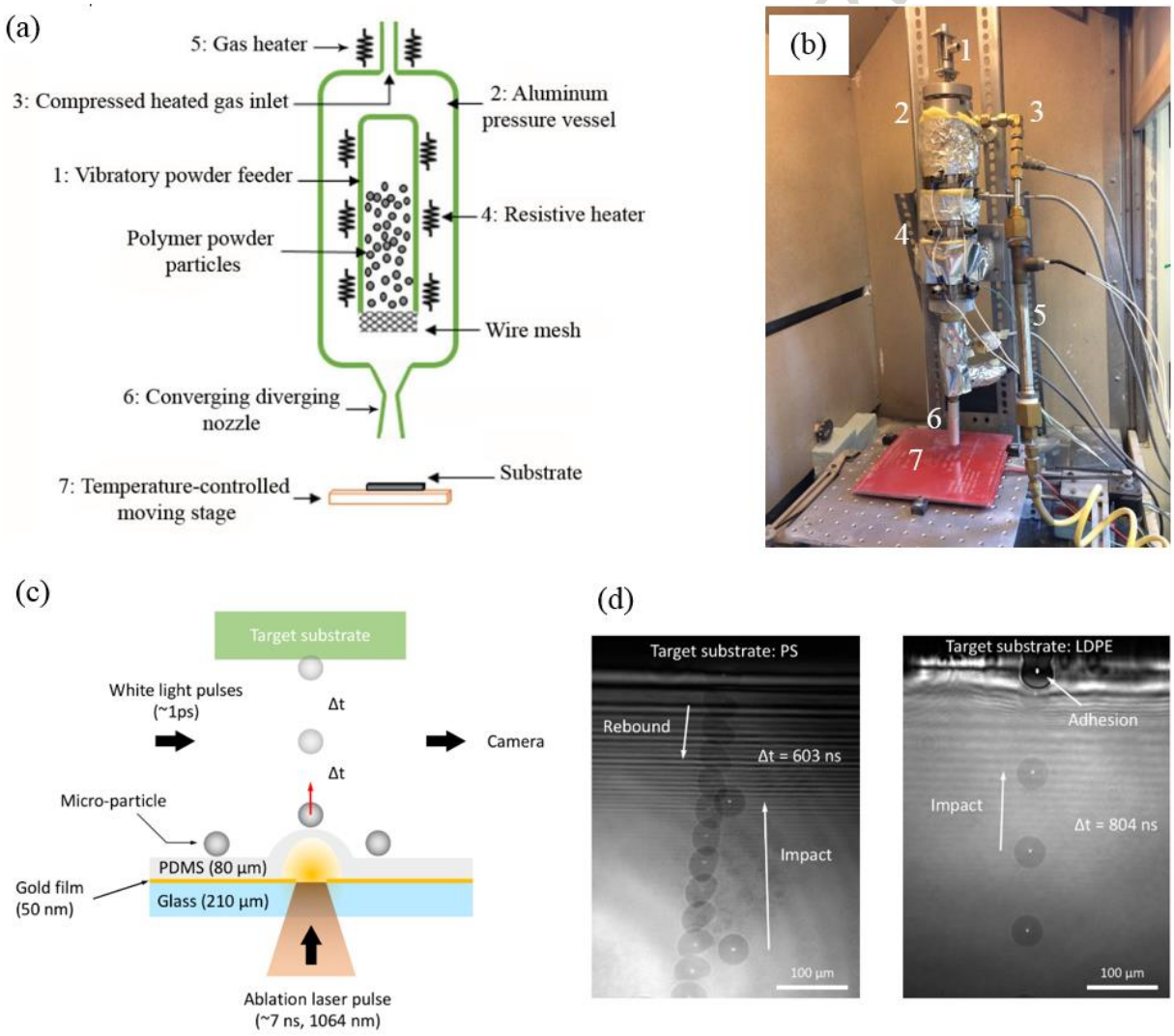

Figure 1 – a) A schematic diagram of the cold spray setup, b) a picture of the cold spray setup used in these experiments, c) a schematic diagram of the single particle impact setup and d) sample ultrafast images of particles approaching and impacting different target substrates.

The material properties of the PA and PS powders and the LDPE substrate studied in this work are presented in Table 1. As can be observed from the SEM images of the feedstock powders in Figure 2, the PS particles are nearly spherical, but the PA are more irregular with facetted surfaces and sharp edges which make them more challenging to process through the hopper of the cold spray system. The original spherical shape of the PS particles also allowed for a study of the plastic deformation for the deposited particles in the micro-ballistic single particle impact experiments because the original, undeformed radius, $r_{0,}$ could be compared against the final, deformed radius, r, of the deposited particle measured normal to the impact direction in order to calculate the resulting compression ratio, $\Delta r / r_0 = (r - r_0) / r_0$, of the PS particles.

Table 1 – Properties of polymer materials studied either as powder particles or substrate

Material	T_g [°C]	T_m [°C]	M_W of the repeat unit [g/mol]	D [µm]	Supplier
LDPE (substrate)	–125	112	28	–	McMaster Carr
PA (powder)	97	180	300	50 ± 25	KU Leuven
PS (powder)	100	175	104	44 ± 4	KU Leuven

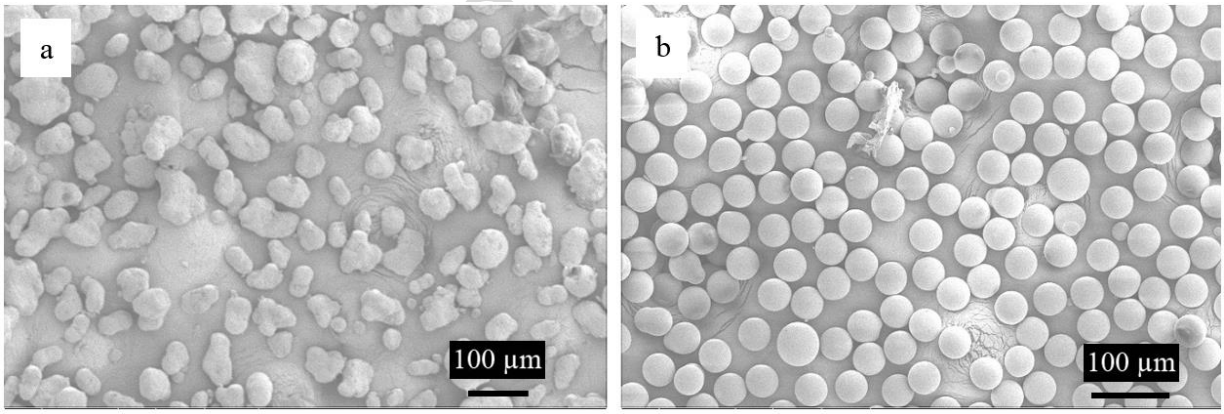

Figure 2 – SEM images of the feedstock powder particles (a) PA and (b) PS.

3. Results and Discussion

A series of cold spray experiments were performed for PS and PA particles deposited on melt-cast PS, PA, and LDPE substrates. In all the experiments, the substrate temperature was fixed at T_s = 100 °C, while the particle temperature and impact velocity were varied so that the deposition window for each particle/substrate combination could be determined. In Figure 3, the deposition windows of PA-on-LDPE, PA-on-PA, PS-on-LDPE and PS-on-PS are shown for the cold spray technique as a function of particle temperature. The lower bounds of the deposition window is defined by the critical particle impact velocity above which deposition of PS and PA particles were found to be possible. This critical particle impact velocity, V_{cr}, is defined independently from deposition efficiency such that any observed deposition, even if it was at an extremely low deposition efficiency, was considered to be successful. As we will discuss later, deposition efficiency was found to improve with increasing impact velocity and, as a result, operation at the critical impact velocity is not the most optimized settings for cold spray deposition. Typical cold spray systems operate at $1.5V_{cr}$.

When depositing on the softer melt-cast LDPE substrate, as seen in Figure 3a and 3c, the critical impact velocity for the PS and PA particles at room temperature was found to be slightly above 160 m/s. As the temperature was increased, the critical velocity was found to decrease roughly linearly with increasing temperature for both the PS and the PA particles to values close to 150 m/s at a particle temperature of T_p =100°C. The same decreasing trend has been observed for cold spray of metals like aluminum, copper and steel for the critical velocity with increasing the particle temperature [25 – 27]. The deposition window for PA and PS on LDPE are similar in some ways. For instance, from Figure 3a and 3c, we note that the critical velocity decays with roughly the same temperature dependence for both the PA and PS particles deposited on LDPE. However, there are some important differences to be pointed out as well. At 120°C and above, the PS particles became tacky inside the powder feeding hopper, making powder delivery difficult and cold spray processing impossible. This did not happen for PA particles which could be processed well above T_p = 120 °C. The other major difference was the existence of an upper velocity limit for PS particles above which particles were found to rebound from the substrate leaving signs of erosion on the surface of the substrate. At room temperature, this upper limit was found to be 230m/s for the PS particles. It was found to increase linearly with increasing

particle temperature resulting in a deposition window that expands with increasing temperature. The PA particles, on the other hand, appeared to deposit on LDPE even at the highest velocities studied in this work. It is possible that an upper limit would have been found for PA if higher velocity experiments were performed, however, here we chose to limit our study to velocities less than the speed of sound, $Ma = 1$, to avoid issues associated with shock waves. This upper limit has been observed before [15], and represents the limit where the incoming particles begin to remove particles that initially adhere through an ablation process.

For the case of like-on-like deposition shown in Figure 3b and 3d, the deposition boundaries were found to shift to higher critical velocity for a given particle temperature creating smaller windows of deposition than those deposited on LDPE. For example, at room temperature, the critical velocity for PA shifted from V_{cr} = 161m/s on LDPE to V_{cr} = 181m/s on PA (Figure 3a and 3b) while the critical velocity for PS shifted from 161m/s on LDPE to 170m/s on PS (Figure 3c and 3d). As the temperature was increased, the critical velocity was found to decay about 1.5 times more rapidly for deposition of PA-on-PA than that of PA-on-LDPE. Interestingly, deposition of PA on both substrates it reached roughly the same critical velocity of about V_{cr} = 155m/s once the particle temperature reached T_p =120 °C. The change in slope between substrates was not as great for the PS but it can still be observed in Figures 3a and 3b resulting in a critical impact velocity of V_{cr} = 155m/s for PS-on-LDPE and V_{cr} = 170m/s for PS-on-PS at a particle temperature T_p =100°C. The observed differences in critical impact velocity between deposition on LDPE and the like-on-like deposition are likely due to the mismatch in the modulus between the particle and substrate. It is well known that a modulus mismatch can lead to an increase in plastic deformation and thus an increased likelihood of adhesion upon impact [15, 21, 28]. The differences observed between the like-on-like deposition of PS and PA were unexpected as both PS and PA have roughly the same T_g and T_m. The differences could be linked to the stronger temperature dependence of the critical impact velocity of the PA particles than that of the PS particles.

From Figure 3 (a – d), an upper limit of deposition can be observed in three of the four deposition windows. Beyond the critical velocities for erosion, particle deposition was initially successful. However, all the polymer particles that initially adhered to the surface were all subsequently stripped from the substrate as the cold spray stream traversed the surface. The

coating failure was always found to occur at the interface between the deposited particles and substrate indicating an adhesive failure induced either by impacting particles dislodging adsorbed particles or the high speed impinging air jet shearing particles from the substrate. For PA particles, the upper limit of deposition was found when the substrate was changed from LDPE to melt-cast PA. Within the range of our experiments, no upper limit was found for PA-on-LDPE deposition. PA-on-PA deposition was found to fail for particle impact velocity above V_i > 210m/s for experiments performed at room temperature. This upper limit of deposition for PA-on-PA was found to increase slightly as the temperature increased reaching a value of V_i = 220m/s at 120°C. For the PS particles, an upper limit of the deposition window was found for both PS-on-PS and PS-on-LDPE depositions, although with slightly different rate of increase in the maximum impact velocity with increasing temperature. The dashed lines which have been superimposed over the deposition data in Figure 3 illustrate the trend of both the lower and upper limits of deposition with increasing temperature. The slope of these trendlines was found to range between 0.23 and 0.33. This is notably smaller than what was previously obtained for the cold spray deposition of HDPE particles on PVC and POM (polyoxymethylene) substrates where slopes were between 0.55 – 0.66 [15]. A similarly weaker temperature dependence of critical velocity for successful deposition of both the PA and PS particles was also observed for cold spray deposition compared to HDPE particles. These differences are likely due to differences in the thermal softening of the different polymers at high temperatures and high deformation rates of impact. Interestingly, the upper velocity limit which

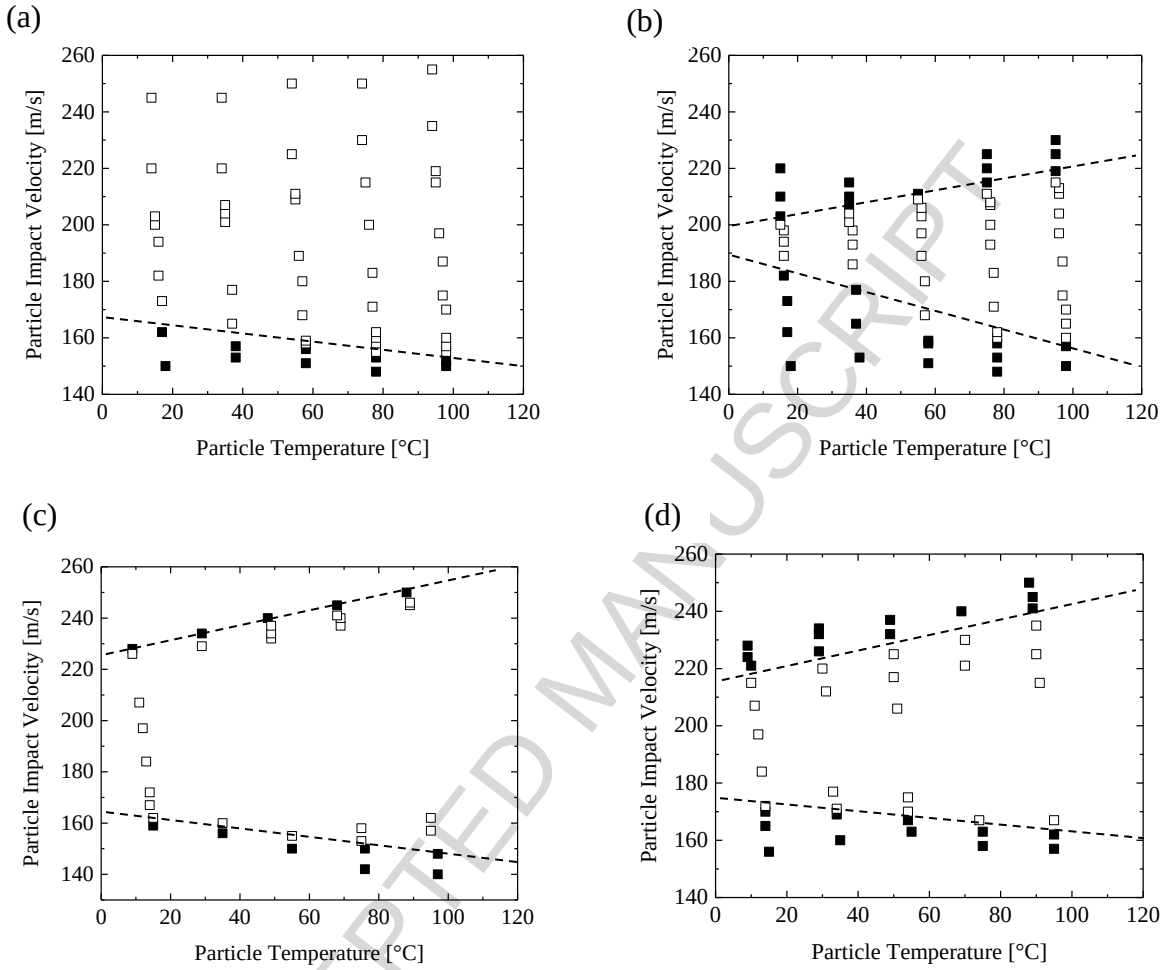

Figure 3 – Deposition window of (a) PA-on-LDPE, (b) PA-on-PA, (c) PS-on-LDPE and (d) PS-on-PS in cold spray experiment showing the transition from no deposition (!) to deposition (□). In all cases, the substrate was held fixed at T_s= 100°C and the stand-off distance was 10mm. Above T_p>120°C, the particles became tacky in the hopper making cold spray impossible.

In order to better understand the window of deposition achieved in cold spray, a series of micro-ballistic single particle impact experiments were performed under experimental conditions designed to mimic those experienced in the cold spray process. In all cases, the particle and substrate temperature were held constant at 100°C while the particle impact velocity was varied from 50 – 500m/s. In each case, the impact velocity was measured from the ultrafast photographs and, in the experiments where adhesion was not observed, the rebound velocity was also

measured. After the successful adhesion experiments, electron microscopy was used to inspect the shape and deformation induced in the particle and substrate.

In Figures 4 and 5, the results from single particle impact experiments are shown. Included in these figures are the rebound velocity, V_r, and the coefficient of restitution, $C_r = V_r/V_i$. Here, V_i is the particle impact velocity and V_r is the particle rebound velocity. For particles that were found to adhere to the surface, $V_r = 0$. In Figure 4, the rebound velocity and the coefficient of restitution are presented for micro-ballistic single particle impacts of PS particles with on an LDPE substrate at 100°C to test the importance of particle size on the results. In these experiments, particle diameters ranging from D_p = 40 to 47μm were studied. Within the particle size range studied, no significant variation was observed on either of the critical velocity or the coefficient of restitution. Similar results were obtained for PA particles depositing on LDPE in single particle impact experiment. The critical velocity obtained for PA particles in the single impact method, did not show significant dependency on particle size even though the variation in PA particles sizes (50 ± 25μm) was significantly larger than PS particles (44 ± 4μm). Thus, particle impact velocity appears to be the most important experimental variable governing particle deposition.

In Figure 5, the results from single particle impact experiments are shown for PS particles impacts on PS and LDPE substrates as well as PA particle impacts on PA and LDPE substrates for varying impact velocity. In Table 2, the critical velocity obtained from both micro-ballistic single particle impact experiments and cold spray process for PS particles depositing on PS and LDPE and PA particles depositing on PA and LDPE is presented for comparison. The particles and substrates were kept at 100°C in both the cold spray and micro-ballistic impact experiments to make comparison possible. It can be seen from the data in Table 2 that the micro-ballistic single impacts of PS particles depositing on LDPE yielded a critical velocity in the range of V_{cr} = 120m/s to 140m/s. This critical velocity compares favorably to the value obtained from the cold spray process, $V_{cr} = 160 \pm 7$m/s. The PA particles started depositing on LDPE at a slightly higher critical velocity range in the single impact experiments, V_{cr} = 170 to 180m/s. Again, this critical velocity compares favorably with the value measured in the cold spray process, $V_{cr} = 150 \pm 30$m/s. The larger standard deviations obtained for critical velocities of PA particles in the cold spray process compared to that of PS particles is due to the wider size distribution of PA

particles ($50 \pm 25\mu m$) compared to that of PS particles ($44 \pm 4\mu m$). This size variation affects the calculation of the impact velocity as the particle velocity is not measured in the cold spray process but predicted from a series from the compressible flow calculations [15], where the particle diameter is an important input parameter.

The coefficient of restitution, $C_r = V_r/V_i$, is plotted against the impact velocity in Figure 5b. The coefficient of restitution, or more appropriately, one minus the square of the coefficient of restitution, $(1 - C_r^2)$, is indicative of the amount of kinetic energy dissipated by the impacting particles. From numerical simulation, it is known that in high speed collisions with velocities above 250 m/s, a large portion of the kinetic energy is dissipated in the form of plastic deformation in regions adjacent to particle/substrate interface [18]. In the case of depositing on LDPE, the coefficient of restitution was found to decrease with increasing the particle impact velocity, V_i, for both PS and PA in micro-ballistic single impact trials until it reached zero at the critical velocity when the particles began to adhere. Above the critical velocity, $C_r = 0$, indicating 100% deposition efficiency for PA and PS particles accelerated onto LDPE substrate through the micro-ballistic impact experiments. This observation also indicates that there is no upper velocity limit, at least, within the range of impact velocities tested here for deposition of PA and PS on LDPE in the single impact trials. This suggests that the impact of successive particles plays a role in the failure to successfully deposit PS and PA on LDPE at large velocities in cold spray. Perhaps the shear stress of successive impacts at a glancing angle is enough to dislodge poorly adhered particles. We will come back to this discussion later in the paper.

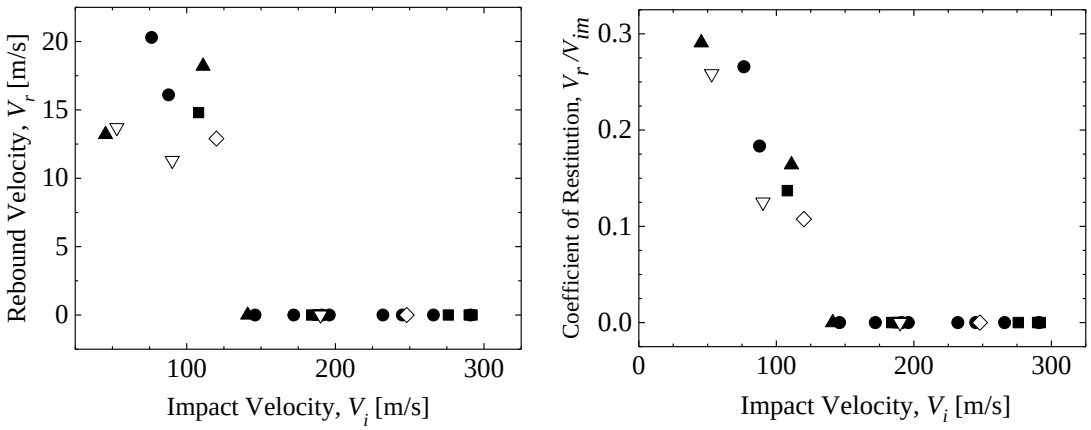

Figure 4 – Results for the micro-ballistic single particle impact experiment including (a) rebound velocity and (b) coefficient of restitution for single particles of polystyrene with the particle size range of 40 – 42µm, (!) , 42 – 43µm, (●), 43 – 44µm, (▲), 44 – 4µm, (∇), 45 – 47µm, (♦), on an LDPE substrate at 100°C.

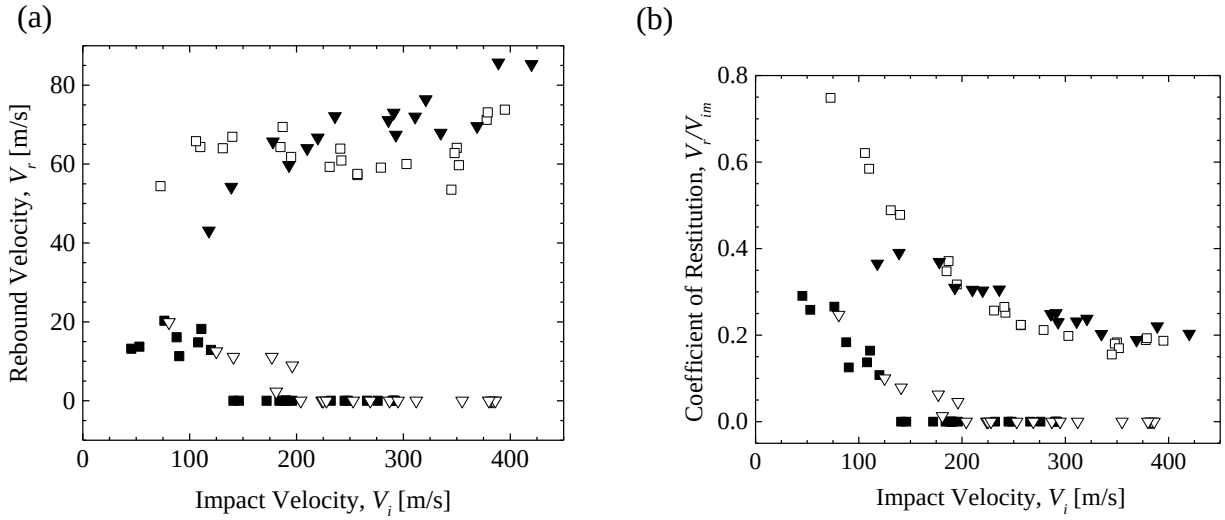

Figure 5 – Results for the micro-ballistic single particle impact experiment including (a) rebound velocity and (b) coefficient of restitution for PS-on-LDPE, (!), PS-on-PS, (□), PA-on-LDPE, (∇), and PA-on-PA, (▼), in the single particle impact test. Both particles and substrates were at the same temperature, $T_p = T_s = 100$°C.

Table 2 – Critical velocity obtained from single particle impact test and cold spray process for PS and PA particles deposited on LDPE and PS or PA substrates. Particle and substrate temperature were kept at 100°C.

Particle and Substrate Materials	Single Particle Impact Test Results	Cold Spray Process Results
PS-on-LDPE	120 – 140m/s	160 ± 7m/s
PA-on-LDPE	170 – 180m/s	150 ± 30m/s
PS-on-PS	No deposition	170 ± 7m/s
PA-on-PA	No deposition	160 ± 30m/s

In the case of micro-ballistic single particle like-on-like deposition, the coefficient of restitution was found to decrease for both the PS and PA particles with increasing impact velocity. The functional form was similar to that observed for impacts on LDPE. However, adhesion was not observed and as a result, the coefficient of restitution never reached zero. Instead, at impact velocities above V_i = 300m/s, the data in the coefficient of restitution plots appeared to approach an asymptotic value of C_r = 0.2 for both the PS and PA particles. Thus, successful like-on-like deposition was not achieved for either PS or PA particles in the micro-ballistic single impact method over the impact velocity range of 100 – 400m/s at 100°C. This represents a major discrepancy between the single particle impact results and the results of the cold spray deposition for which particle adhesion was achieved in like-on-like deposition above a critical velocity of approximately V_{cr} = 170m/s for both PS and PA.

For particles that do adhere to the substrate, SEM can be used to study their final shape and degree of deformation. A series of SEM images of PA particles absorbed on the LDPE substrate following micro-ballistic single particle impact at 100°C are shown in

Figure 6. All of the SEM images presented in

Figure 6 were at an angle of 80°. Some evidences of melting of the particles can be observed at the interface connecting the particle to the substrate where the surface roughness of the particle clearly changes from rough to smooth. As the impact velocity was increased, the degree of polymer melting, and flow clearly increased with liquid regions appearing to flow or

climb up the side of the particle after or during deposition. During impact the particle deforms the interface. If the particle or substrate locally melts, it could be pulled back up with the particle as some of the deformation is elastically recovered. It is not clear, however, if the melting originates from the particle or from the substrate. It is likely that the majority of the melt polymer has originated from the substrate rather than the particle because the melting point of LDPE is more than 50°C less than that of PA. However, recent numerical simulations have shown that upon impact, the temperature at the interface should exceed the melting temperatures of both LDPE and PA [21]. If the melting did indeed originate from the substrate, then it follows that any volume of LDPE from the substrate that has wetted onto the particle, must have been displaced from the substrate leaving behind a crater. However, because no crater is visible adjacent to the deposited particles, any LDPE polymer present on the impacted particle must have been displaced from just beneath the particle. It is likely that the flow of the substrate material onto the particles is contributing to the particle/substrate bond.

The SEM images of PS single particles deposited on LDPE in the micro-ballistic experiment at different impact velocities are shown in Figure 7. Although significant differences are not observed between these SEM images in Figure 7(a – c) at various impact velocities, a small increasing trend is noticeable in the plastic deformation of the PS particles with increasing the impact velocity. Evidence of melting is also visible around the PS particle deposited on LDPE, more noticeably in Figure 7c at an impact velocity of V_i = 290m/s. The presence of the clear melted region might help explain the difference between the like-on-like and particle on LDPE results. LDPE is well above its T_g at the processing temperature and its melt temperature, T_m = 110 °C is just above the process temperature. As a result, local melting of the LDPE at the particle substrate interface is likely. This molten region likely helps dissipate energy and increase adhesion strength. For both the PS and PA particles, the melting temperature is well above the processing conditions and as a result melting is unlikely.

The plastic deformation measured following the successful deposition of the PS particles onto an LDPE substrate using the micro-ballistic single impact technique experiments are plotted against particle impact velocity in

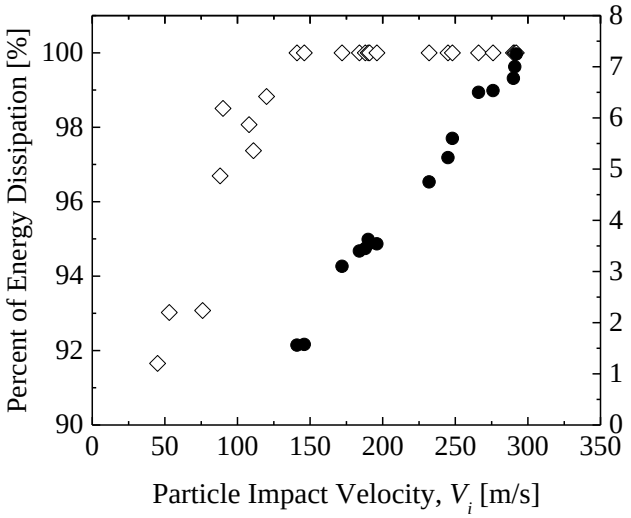

Figure 8. The plastic deformation of the particles was found to increase linearly with increasing impact velocity. Similar linear trends were observed between the plastic deformation and the impact velocity for aluminum particles depositing on either sapphire or aluminum in laser-induced single particle impact experiments [24, 29]. Unfortunately, the plastic deformation could not be quantified for the PA particles because, unlike the PS particles, they did not begin the experiment spherical and, as a result, it is unclear what initial condition the final deformed particle should be compared to in order to determine the plastic deformation.

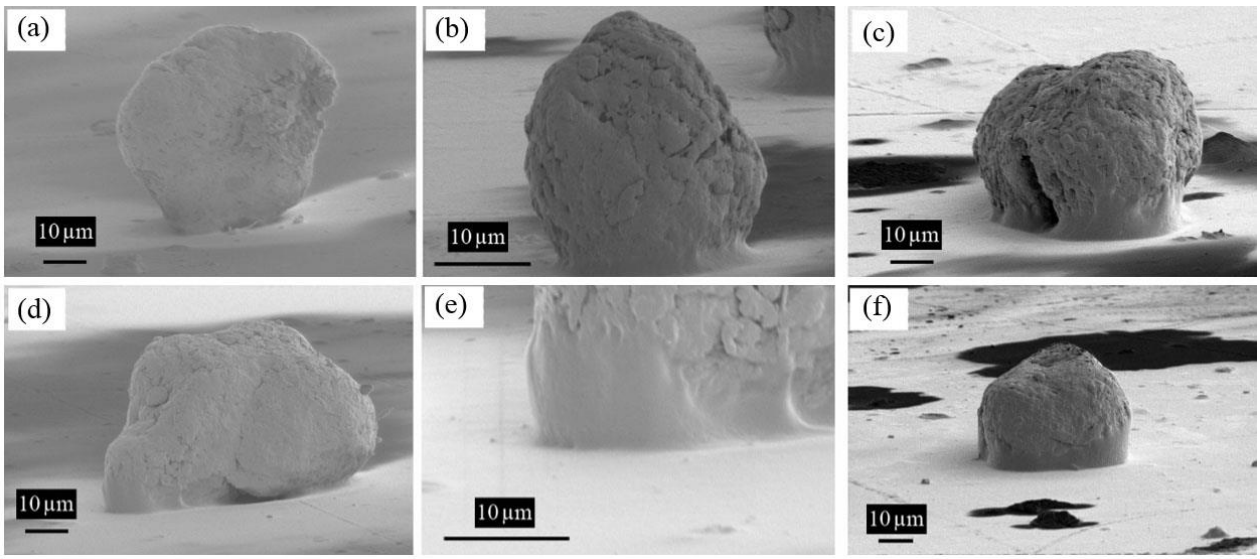

Figure 6 – SEM images of PA particles deposited on LDPE through a micro-ballistic impact experiment. The data include particles with impact velocities of a) V_i = 225m/s, b) 295m/s, c) 355m/s, d) 382m/s, e) higher magnification imaging of (d), and f) 384m/s. All experiments were performed at 100°C. All images are taken at 80° angle so that the interface between particle and substrate could be observed.

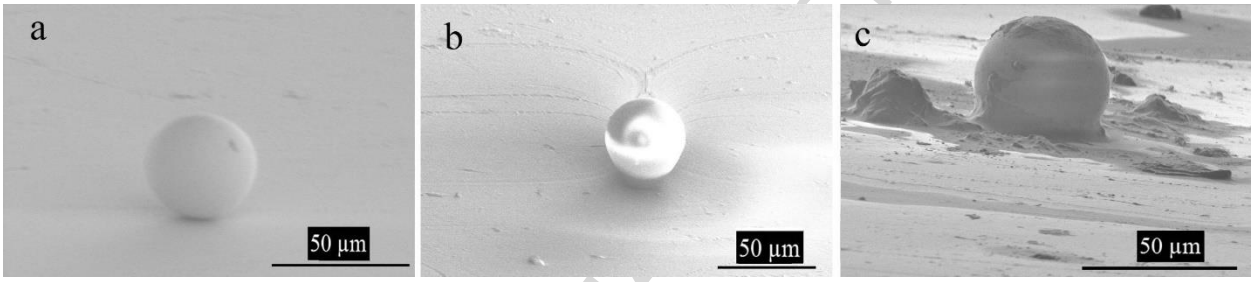

Figure 7 – SEM images of the individual particles of polystyrene deposited on a LDPE substrate at impact velocities of a) V_i = 140m/s, b) 230m/s, c) 290m/s. Both particles and substrates were at a temperature of $T_p = T_s$ = 100°C.

The coefficient of restitution was used to infer the total energy dissipated for both the rebounding and adhering particles, (1 - C_r^2), and it is included in

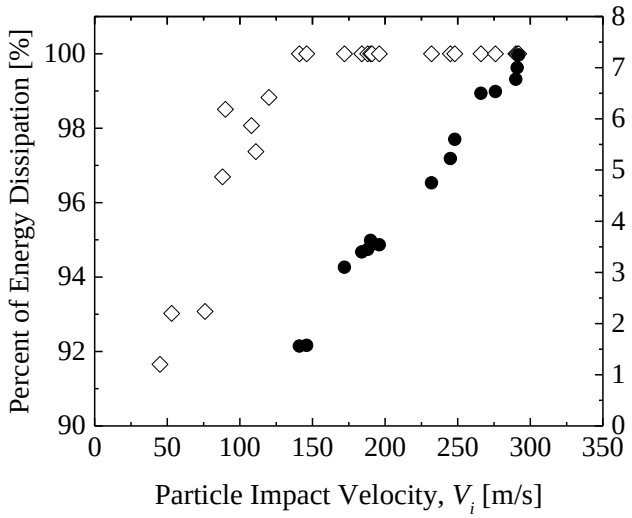

Figure 8 to provide a direct comparison to plastic deformation data of the PS particles. For PS-on-LDPE, at impact velocities as low as V_i = 50m/s, the percentage of impact energy dissipation was above 90%. With increasing impact velocity, the dissipated portion of the impact energy was found to increase monotonically until it reached 100% at V_i = 140m/s. SEM images of the PS particles deposited on LDPE in the micro-ballistic single particle experiments were analyzed using a software, ImageJ to measure the radius, r, of the PS particle perpendicular to the substrate surface. The results were compared to the initial diameter, $r_{0,}$ of the PS particle known from the ultrafast photography before impact.

The plastic deformation of the PS particles deposited on the LDPE substrate in the micro-ballistic single particle impacts was studied using the SEM images. The compression ratio of the particle needed for deposition of PS-on-LDPE in the single particle impact method was measured to be $\Delta r/r_0$ = 1.5%. Here, local strains which should clearly be much larger than this at the interface between the particle and the substrate and not be directly measured. The numerical simulation of Shah et al. [21] for the impact of high density polyethylene (HDPE) particles on a HDPE substrate at room temperature showed that the compression ratio of the particle increases

from 0.5% at impact velocity of V_i =150m/s to 1.5% at the impact velocity of V_i = 250m/s. This suggests that giving similar compression ratios that it is reasonable to use these simulations to probe in more details of the deformation and temperature history of the particles and infer similar trend in our experimental impacts. Meanwhile, in the simulations of Shah et al. [21] the temperature at the particle/substrate interfacial region was shown to increase from 32°C to 47°C when the impact velocity was increased from V_i = 150 to 250m/s. The present single impact study for PS particles impacting on an LDPE substrate indicated an increase in compression ratio from 1.5% at the impact velocity of V_i = 140m/s to 7.2% at the impact velocity of V_i = 295m/s. Wanting et al. [24] studied the laser induced single particle impact of aluminum particles with an average diameter of D_{ave} = 19μm on sapphire and found an increase in the plastic deformation of the particles from $\Delta r/r_0$ = 15% to $\Delta r/r_0$ = 55% with increasing the impact velocity from V_i = 170m/s to V_i = 700m/s. Thus, the compression ratio we obtained here in the micro-ballistic single impact experiments for the PS particles on LDPE is an order of magnitude less than that of aluminum particles depositing on sapphire in a similar deposition technique. This implies another important difference between metals and polymers when applying these additive manufacturing techniques.

The cold spray deposition efficiency, *DE*, of PA-on LDPE, PS-on-LDPE, PA-on-PA and PS-on-PS is plotted against particle impact velocity in Figure 9. The deposition is quantified by measuring the change in mass of the substrate after deposition and comparing that to the mass of powder used during the experiment. The deposition efficiency of the PA particles was found to be larger than that of the PS particles for both the case of cold spray deposition on LDPE and the case of like-on-like deposition. These differences are likely due to the variations of their mechanical and viscoelastic properties at elevated temperatures and extremely high shear rates. In Figure 9, a monotonic increase in the deposition efficiency is observed with increasing the impact velocity of the PA and PS particles in both like-on-like deposition cases and deposition on LDPE. With increasing impact velocity, however, the deposition efficiency was not found to increase past 5% for any of the velocities or any of the studied particle-substrate combinations. For metals like copper and aluminum, on the other hand, the variation of deposition efficiency deposition efficiency with particle impact velocity is reported to be quite different [2]. They resemble more like a step function rather than a continuous trend observed here. In metal cold

spray, at impact velocities just above the critical velocity, a deposition efficiency of DE = 25% is observed, but then it abruptly increases to DE = 75 – 100% at impact velocities higher than $1.2V_{cr}$ [2]. A similar trend was not observed here or for HDPE depositions in the past [15].

The results of the single particle impacts, however, showed a 100% deposition for the roughly 25 trials of particles impacting the LDPE substrate at velocities above the critical velocity. One possible reason for the differences between deposition efficiency of cold spray and that of micro-ballistic single impacts could be that the successive impacts might be dislodging the initially deposited particles. The roughness of the substrate surface can also play a role in determining the deposition efficiency. In the cold spray process, only the first layer of particles hit the smooth surface of the substrate and thereafter all other incoming particles impacted on the rough and bumpy surface of an already deposited layer of particles. This was not the case for the single particle impact experiments because secondary impacts were not examined and the single particle was impacted on the smooth substrate surface rather than deposited particles.

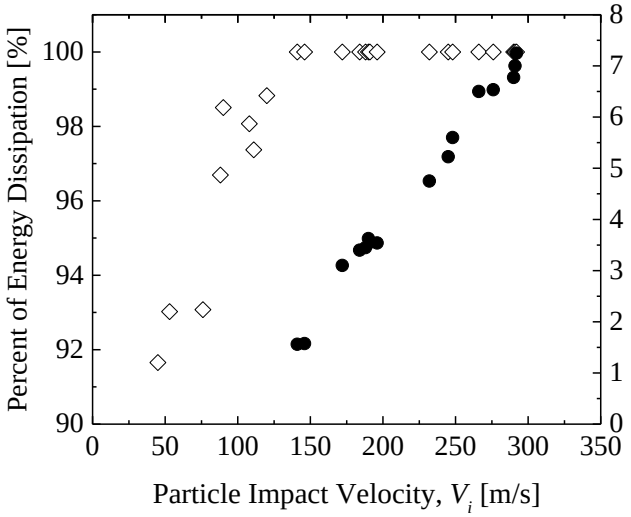

Figure 8 – Results for the micro-ballistic single particle impact experiment including the plastic deformation (●) and percent of energy dissipation upon impact (♦) for PS particles accelerated toward the LDPE substrate. All experiments were performed at 100°C.

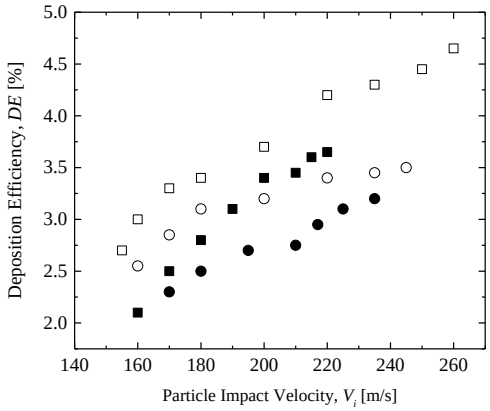

Figure 9 – Deposition efficiency as a function of particle impact velocity for PA-on-LDPE (□), PA-on-PA (!), PS-on-LDPE (○), and PS-on-PS (●), in the cold spray process. Both particle and substrate were at $T_p = T_s$ =100°C.

The reasons behind the successful like-on-like deposition observed for cold spray of PS and PA and the failure to obtain successful deposition for micro-ballistic single impacts may also stem from multiple impacts; either successive or simultaneous. Multiple impacts, if head on or nearly head on, can produce extra plastic deformation and melting in the initially deposited primary particle. Thus, it seems reasonable that multiple particle strikes can be either advantageous or disadvantageous depending on the angle of impact. If the secondary particle collides simultaneous with the primary particle, it could increase the likelihood of adhesion of the primary particle by increasing the primary particle deformation upon impact. If the secondary particle collides after the primary has already adhered to the substrate it might still be beneficial as it could induce additional deformation through peening that could improve the strength of the primary particle/substrate adhesion making the primary particle less susceptible to the detrimental effects of an impact at a more acute angle which could dislodge a weakly adhered particle. Ganesan et al. [9] also confirmed the significance of the peening effect of secondary particles in the formation of a uniform coating on a polymeric substrate.

For simultaneous particle impacts to play a key role in the cold spray deposition process of polymers, there must be a non-zero probability of a second particle hitting the first particle within the time it is impacting the substrate. This impact time has been calculated to be about 30 ns [21]. In order to assess this possibility, take for example, a specific set of process conditions in which the impact velocity of particles is 200m/s, the standoff distance from the nozzle exit is 10

mm, the particle flowrate is 50g/min, and the mean particle size is 40μm. Under these conditions, the probability of second particle striking the primary particle during its impact can be approximated to be about 1%. Although not large, this probability of hitting in cold spray is significant enough that it is reasonable to assert that simultaneous multi-body impact could be playing a role in explaining the difference between these two methods. It is also important to note that in cold spray, the deposition efficiency was found to increase with increasing flowrate of particles up to a limit of 50g/min. Finally, we should note that the peening effect of other particles and their bombardment on an already impacted particle as well as reducing the roughness of the substrate can affect the particle/substrate bonding process.

4. Conclusions

In this work, we utilized a laboratory-scale cold spray setup to deposit PA and PS either on LDPE or on melt cast substrates of PA and PS. Variation of the critical velocity was studied with increasing particle temperature which helped developing deposition maps for the four particle/substrate combinations studied in this work. A series of laser induced micro-ballistic single particle impact experiments were also conducted using the same materials as powder particle or substrate and the results were compared to those of the cold spray process. For the cases where polymer particles were deposited on LDPE, both methods yielded roughly similar critical velocities for both PA and PS particles. The cold spray process yielded a critical velocity of V_{cr} = 160 ± 7m/s and 150 ± 30m/s for PS-on-LDPE and PA-on-LDPE depositions, respectively. The micro-ballistic single particle impact method, on the other hand, measured the critical velocity in the V_{cr} = 120 – 140m/s and 170 – 180m/s ranges for PS-on-LDPE and PA-on-LDPE depositions, respectively. However, there appeared to be several important differences between the single particle impact experiment and the cold spray process. The deposition efficiency did not exceed 5% in the cold spray process whereas in the micro-ballistic single particle impact method 100% deposition efficiency was achieved at impact velocities above the critical velocity. Unlike the cold spray process, in single particle impact, the effect of successive particle collisions on the first deposited particle as well as the effect of airflow is eliminated. The enhanced plastic deformation in both the primary particle and the substrate beneath the primary particle due to the successive head on particle collisions might explain why we achieved like-on-like deposition in the cold spray process but not in the micro-ballistic single particle impacts. The plastic deformation in micro-ballistic single particle impacts was measured for PS particles depositing on LDPE from SEM studies and was found to be comparable to the simulation results for cold spray of polymers. However, compared to metals, the plastic deformation of the studied polymers in the micro-ballistic single particle impact experiments was an order of magnitude smaller than that of metals depositing on sapphire in a same process but at considerably higher impact velocities. Finally, the cold spray process showed a monotonic increase in deposition efficiency of the studied polymer materials with the impact velocity which is quite different from that of metals which more looks like a step function.

Acknowledgments

This research was accomplished through a cooperative research agreement with the US Army Research Laboratory, Contract: W911NF-15-2-0024, “Intelligent Processing of Materials by Design”. The authors would also like to thank Peter Van Puyvelde of KU Leuven for supplying the polystyrene and polyamide particles used in these studies.

References

[1] A. Papyrin, V. Kosarev, S. Klinkov, A. Alkhimov, V.M. Fomin, Cold Spray Technology, Amsterdam: Elsevier, 2007.

[2] H. Assadi, T. Schmidt, H. Richter, J.-O. Kliemann, K. Binder, F. Gartner, T. Klassen, H. Kreye, "On Parameter Selection in Cold Spraying," *Thermal Spray Technology,* vol. 20, no. 6, pp. 1161-1176, 2011.

[3] M. Gardon, A. Latorre, M. Torrell, S. Dosta, J. Fernandez, J.M. Guilemany, "Cold Gas Spray Titanium Coatings onto a Biocompatible Polymer," *Materials Letter,* vol. 106, pp. 97-99, 2013.

[4] X.L. Zhou, A.F. Chen, J.C. Liu, X.K. Wu, J.S. Zhang, "Preparation of metallic coatings on polymer matrix composites by cold spray," *Surface & Coatings Technology,* vol. 206, no. 1, p. 132–136, 2011.

[5] A.M. Vilardell, N. Cinca, A. Concustell, S. Dosta, I.G. Cano, J.M. Guilemany, "Cold spray as an emerging technology for biocompatible and antibacterial coatings: state of art," *Materials Science,* vol. 50, no. 13, p. 4441–4462, 2015.

[6] H. Assadi, H. Kreye, F. Gartner, T. Klassen, "Cold spraying: A materials perspective," *Acta Materialia,* vol. 116, pp. 382-407, 2016.

[7] V.K. Champagne, D. Helfritch, P. Leyman, S. Grendahl, B. Klotz, "Interface Material Mixing Formed by the Deposition of Copper on Aluminum by Means of the Cold Spray Process," *Thermal Spray Technology,* vol. 14, no. 3, pp. 330-334, 2005.

[8] V. Champagne, The Cold Spray Materials Deposition Process: Fundamentals and Applications, Woodhead Publishing, Cambridge: Woodhead Publishing, 2007.

[9] A. Ganesan, J. Affi, M. Yamada, M. Fukumoto, "Bonding behavior studies of cold sprayed copper coating on the PVC polymer substrate," *Surface & Coatings Technology,* vol. 207, p. 262–269, 2012.

[10] R. Lupoia, C. Stensona, K.A. McDonnellb, D.P. Dowlingb, E. Ahearne, "Antifouling coatings made with Cold Spray onto polymers: Process characterization," *CIRP Annals - Manufacturing Technology,*

vol. 65, p. 545–548, 2016.

[11] G. Archambault, B. Jodoin, S. Gaydos, M. Yandouzi, "Metallization of carbon fiber reinforced polymer composite by cold spray and lay-up molding processes," *Surface & Coatings Technology,* vol. 300, p. 78–86, 2016.

[12] A.S. Alhulaifi, G.A. Buck, W.J. Arbegast, "Numerical and Experimental Investigation of Cold Spray Gas Dynamic Effects for Polymer Coating," *Thermal Spray Technology,* vol. 21, pp. 852-862, 2012.

[13] K. Ravi, Y. Ichikawa, T. Deplancke, K. Ogawa, O. Lame, J.-Y. Cavaille, "Development of Ultra-High Molecular Weight Polyethylene (UHMWPE) Coating by Cold Spray Technique," *Thermal Spray Technology,* vol. 24, no. 6, p. 1015–1025, 2015.

[14] Y. Xu, I. M. Hutchings, "Cold spray deposition of thermoplastic powder," *Surface & Coatings Technology,* vol. 201, no. 6, p. 3044–3050, 2006.

[15] T.P. Bush, Z. Khalkhali, V.K. Champagne, D.P. Schmidt, J.P. Rothstein, "Optimization of Cold Spray Deposition of High-Density Polyethylene Powders," *Thermal Spray Technology,* vol. 26, no. 7, p. 1548–1564, 2017.

[16] H. Che, P. Vo, S. Yue, "Metallization of carbon fibre reinforced polymers by cold spray," *Surface & Coatings Technology,* vol. 313, p. 236–247, 2017.

[17] F. Meng, D. Hu, Y. Gao, S. Yue, J. Song, "Cold-spray bonding mechanisms and deposition efficiency prediction for particle/substrate with distinct deformability," *Materials and Design,* vol. 109, p. 503–510, 2016.

[18] M. Grujicic, J.R. Saylor, D.E. Beasley, W.S. DeRosset, D. Helfritch, "Computational analysis of the interfacial bonding between feed-powder particles and the substrate in the cold-gas dynamic-spray process," *Applied Surface Science,* vol. 219, pp. 211-227, 2003.

[19] M. Grujicic, C.L. Zhao, W.S. DeRosset, D. Helfritch, "Adiabatic shear instability based mechanism for particles/substrate bonding in the cold-gas dynamic-spray process," *Materials and Design,* vol. 25, no. 8, p. 681–688, 2004.

[20] T. Hussain, "Cold Spraying of Titanium: A Review of Bonding Mechanisms, Microstructure and Properties," *Key Engineering Materials,* vol. 533, no. ISSN: 1662-9795, pp. 53-79, 2012.

[21] S. Shah, J. Lee, J.P. Rothstein, "Numerical Simulations of the High Velocity Impact of a Single Polymer Particle during Cold Spray Deposition," *Thermal Spray Technology,* vol. 26, no. 5, pp. 970-984, 2017.

[22] A. Shapiro, The Dynamics and Thermodynamics of Compressible Fluid Flow, The Ronald Press Company, 1953.

[23] V.K. Champagne, D.J. Helfritch, S.P.G. Dinavahi, P.F. Leyman, "Theoretical and Experimental Particle Velocity in Cold Spray," *Thermal Spray Technology,* vol. 20, p. 425–431, 2011.

[24] W. Xie, A.A. Dehkharghani, Q. Chen, V.K. Champagne, X. Wang, A. T. Nardi, S. Kooi, S. Müftü, J.-H. Lee, "Dynamics and extreme plasticity of metallic microparticles in supersonic collisions," *Scientific Reports,* vol. 7, no. 5073, pp. 1-9, 2017.

[25] H. Assadi, F. Gartner, T. Stoltenhoff, H. Kreye, "Bonding Mechanism in Cold Gas Spraying," *Acta Materialia,* vol. 51, no. 15, pp. 4379-4394, 2003.

[26] T. Schmidt, F. Gartner, H. Assadi, H. Kreye, "Development of a Generalized Parameter Window for Cold spray Deposition," *Acta Materialia,* vol. 56, no. 3, pp. 729-742, 2006.

[27] A.S. Alhulaifi, G.A. Buck, W.J. Arbegast, "Numerical and Experimental Investigation of Cold Spray Gas Dynamic Effects for Polymer Coating," *Thermal Spray Technology,* vol. 21, no. 5, p. 852–862, 2012.

[28] G. Bae, Y. Xiong, S. Kumar, K. Kang, C. Lee, "General Aspects of Interface Bonding in Kinetic Sprayed Coatings," *Acta Materialia,* vol. 17, pp. 4858-4868, 2008.

[29] Q. Chen, A. Alizadeh, W. Xie, X. Wang, V.K. Champagne, A. Gouldstone, J.-H. Lee, S. Muftu, "High-Strain-Rate Material Behavior and Adiabatic Material Instability in Impact of Micron-Scale Al-6061 Particles," *Thermal Spray Technology,* vol. 27, no. 4, pp. 641-653, 2018.

Highlights

- Windows of deposition over the velocity and temperature space were developed for polystyrene and polyamide particles in the cold spray technique.
- A set of laser-induced single particle impact experiments were carried out as well for these two materials and the results were compared to that of the cold spray process.
- The critical velocity was slightly different for the two techniques.
- The peening effect of the multiple particles in the cold spray process was proven to encourage bonding.
- SEM analysis revealed the important role of interfacial melting in the formation of a strong particle/substrate bond.